

Autophagy modulation altered differentiation capacity of CD146+ cells toward endothelial cells, pericytes, and cardiomyocytes

Mehdi Hassanpour

Tabriz University of Medical Sciences

Jafar Rezaie

Urmia University of Medical Sciences

Masoud Darabi

Tabriz University of Medical Sciences

Amirataollah Hiradfar

Tabriz University of Medical Sciences

Reza Rahbarghazi (✉ rezarahbardvm@gmail.com)

Tabriz University of Medical Sciences <https://orcid.org/0000-0003-3864-9166>

Mohammad Nouri

Tabriz University of Medical Sciences

Research

Keywords: Human Bone Marrow CD146+ Cells; Autophagy Modulation; Nitrosative assay; lineage-specific differentiation; Exosome activity

Posted Date: February 14th, 2020

DOI: <https://doi.org/10.21203/rs.2.23514/v1>

License: © ⓘ This work is licensed under a Creative Commons Attribution 4.0 International License.

[Read Full License](#)

Version of Record: A version of this preprint was published at Stem Cell Research & Therapy on March 26th, 2020. See the published version at <https://doi.org/10.1186/s13287-020-01656-0>.

Abstract

Background: To date, many attempts are employed to increase the regenerative potential of stem cells. In this study, we evaluated the hypothesis whether an autophagy modulation could induce/reduce CD146⁺ cells differentiation into mature pericyte, endothelial and cardiomyocyte lineage.

Methods In this study, CD146⁺ cells were enriched from human bone marrow aspirates and trans-differentiated into mature EC, PC and CM after exposure to autophagy stimulator (50 μ M Met)/inhibitor (15 μ M HCQ). The protein levels of autophagy proteins were monitored by western blotting. NO content was measured using the Griess assay. Using real-time PCR assay and western blotting, we monitored the lineage protein and gene levels. The fatty acid change was determined by gas chromatography. Pro-inflammatory cytokine and angiocrine factors were measured by ELISA. The exosome secretion capacity was assessed by AChE activity and real-time PCR assay.

Result Data revealed the modulation of autophagy factors, Beclin-1, P62 and LC3 II/I ratio in differentiating CD146⁺ cells after exposure to Met and HCQ ($p < 0.05$). The inhibition of autophagy increased released NO content and decreased intracellular NO content compared to the Met-treated cells ($p < 0.05$). Real-time PCR analysis showed that the treatment of CD146⁺ cells with autophagy modulators altered the expression of VE-cadherin, cTnI and α -SMA. Our data demonstrated that the stimulation of autophagy signaling in CD146⁺ cells with Met increased the expression of VE-cadherin, α -SMA, and cTnI compared to HCQ-treated cells ($p < 0.05$) while western blotting revealed the protein synthesis of all lineage-specific proteins in under the stimulation and inhibition of autophagy. Fatty acid profile analysis revealed the increase of unsaturated fatty acids after exposure to HCQ ($p < 0.05$). None statistically significant differences were found in the levels of Tie-1, Tie-2, VEGFR-1 and VEGFR-2 after autophagy modulation. The treatment of cells with HCQ increased the levels of TNF- α and IL-6 compared to the Met-treated cells. Data revealed the increase of exosome biogenesis and secretion to the supernatant in cells treated with HCQ compared to the Met groups ($p < 0.05$).

Conclusions

In summary, autophagy modulation could be altered differentiation potency of CD146⁺ cells and could be novel and applicable cardiac cell therapy in the cardiac regeneration field.

1. Background

According to WHO statistics, coronary heart disease is the main cause of human mortality in clinical settings. Despite current advances in the decrease mortality rate in patients with coronary heart disease, further attempts and novel approaches are highly needed for the alleviation of cardiac tissue injuries [1]. Up to date, the advent of cell therapy and regenerative medicine is touted as the modern therapeutic procedures in the field of cardiovascular disease [2]. Hitherto, different types of stem cells, including embryonic stem cells, cardiac progenitor cells, mesenchymal stem cells, endothelial progenitor cells, and

induced pluripotent stem cells have been used in the clinical setting. Recently, it has been documented that PCs have great regenerative potential in limb ischemia and myocardial infarction [3, 4]. PCs are a specific population that concentrically wrap vascular ECs [5]. According to recent data, a fraction of PCs exhibits extremely proliferation, and clonogenic capacity with a magnificent stemness feature, pleiotropic properties, and angiogenic potency [6]. Based on molecular analyses, multiple pericyte populations have the potential to express OCT4, NANOG and SOX2, CD146, alkaline phosphatase, CD44, CD73, CD90, and CD105, etc. [7]. The ability of PCs to express CD146 (melanoma cell adhesion molecules) was shown before which contributes to highly proliferative rate differentiation capacity [8]. According to previously published experiments, cardiac tissue encompasses a large number of CD146⁺ cells inside myocardium with a trilineage potential capacity to rescue angiogenesis and replace damaged myocardium [9]. Cardiac PCs are potent to release tissue metalloproteinases to re-model the fibrous matrix in the periphery of the injured sites [10]. These features make PCs as an appropriate cell source for the alleviation of cardiac tissue injuries.

Autophagy is an intricate intracellular process that facilitates the degradation of impaired proteins and the removal of dysfunctional organelles by fusion to lysosomes and releases out of the cell. In addition to the integrity of autophagy to the bioactivity of the host cells, novel data highlighted the interaction and interplay of the autophagy signaling pathway with another signaling cascade reciprocally [11]. Scientific literature demonstrated that autophagy functions in the developmental and maturation of B lymphocytes, adipocytes, osteoblasts, keratinocytes and erythrocytes [12–16]. Interestingly, it was revealed that autophagy inhibition resulted in ROS accumulation in hematopoietic stem cells and self-renewal capacity loss [17]. Zhang et al. showed that the promotion of autophagy in cardiac progenitor cells, done after inhibition of the fibroblast growth factor signaling pathway, accelerated differentiation toward mature CMs, showing the critical role of autophagy in stem cells differentiation properties [18].

Despite PCs significance in hemostasis, angiogenesis, vasculogenesis, differentiation, and maturation into several cardiac cells, there is no information related to the modulation of autophagy on the differentiation potential of immature PCs. In this study, we further evaluated the hypothesis, whether an autophagy modulation could induce/reduce the PC differentiation into mature PCs, ECs and, CMs.

2. Methods

2.1. Mononuclear cells isolation and expansion protocol

Bone marrow samples of healthy volunteers, ranging from 3 to 10 years old, referred to children hospital, an affiliated hospital to Tabriz University of Medical Sciences, were enrolled in the present study. Informed consent was obtained from candidates. Briefly, bone marrow aspirates (2 ml) were used for the isolation of MNCs. In order to inhibit the coagulation, 5,000 IU/mL heparin was used. Blood samples were diluted with PBS (1:1 v/v) and overlaid on the same volume of Ficoll-Hypaque solution (Cat No: GE17-1440-02; Sigma-Aldrich). The samples were centrifuged at 400 g for 25 minutes at 4 °C. MNCs at the interface fraction between the plasma and the Ficoll solution was carefully collected, washed with PBS

and re-suspended in DMEM/LG (Cat No: 31600083; Gibco; USA) culture medium. The media were supplemented with %10 FBS (Cat No: 10270; Invitrogen). The medium was replaced every 3–4 days. By using 0.25% Trypsin-EDTA (Cat No: 25200056; Gibco; USA) solution, cells were detached.

2.2. Enrichment of CD146⁺ cells using Magnetic Activated Cell Sorting

In the current study, we aimed to isolate CD146⁺ cells for different analyses. For this purpose, expanded bone marrow MNCs were detached using the enzymatic solution and subjected to MACS. In short, the MNCs were blocked by using 1% bovine serum albumin for 20–30 minutes and incubated with mouse anti-human CD146 microbead (Order no: 130-093-596; Miltenyi Biotec; Germany) for 30 minutes at 4°C. The cell suspensions were passed over the MACS LS column (Order no: 130-042-401; Miltenyi Biotec).

2.3. Cell survival assay

This study aimed to evaluate the effect of autophagy modulation on the differentiation capacity of CD146⁺ cells toward different lineages. In this regard, we performed MTT assay to select the maximum dose of autophagy blocker, HCQ, with the lowest toxic effect on CD146⁺ cells. In this regard, CD146⁺ cells were plated (2×10^4 /well) in each well of 96-well plates (SPL). Cells were treated with different concentrations of HCQ (Cat No: H0915; Sigma-Aldrich) including 2.5, 5, 10, 15 and 20 μ M for 72 hours [19]. Thereafter, 30 μ l MTT solution was added to each well and incubated at 37°C for 2 hours followed by the addition of 200 μ l dimethyl sulfoxide (Merck; Germany). The optical density was read at 620 nm by using a microplate reader (BioTek). The cell survival rate was expressed as a percentage relative to the non-treated control CD146⁺ cells. In order to stimulate autophagy, CD146⁺ cells were treated with 50 mM Met (As a gift from Osveh pharmaceutical Inc., Tehran, Iran) [20].

2.4. LysoTracker assay

To assess the inhibitory effect of HCQ on the late stage of autophagy, we performed LysoTracker assay. To this end, MNCs were seeded at a density of 10^4 cells per well in 8-well Chambered Cell Culture Slide (SPL) and incubated at 37 °C with 5% CO₂ and 95% relative humidity. After 24 hours, cells were treated with 15 and 20 μ M HCQ for 72 hours. After completion of autophagy modulation, cells were washed with cold PBS, and 50 nM LysoTracker Green (Cat No: L7526; Sigma-Aldrich) was added to each well. Cells were allowed to maintain for 30 minutes. After three times washing with PBS, cells were stained with 1 μ g/ml DAPI (Sigma-Aldrich) solution 30 seconds in order to stain background. The cells harboring intracellular vacuoles were visualized by using immunofluorescence microscopy (Model: BX41; Olympus).

2.5. Cell differentiation and autophagy modulation

In this study, we explored the effect of autophagy modulation on the differentiation potency of CD146⁺ cells in vitro. Purified CD146⁺ cells were cultured in the endothelium (Cat No: C-22111, Promocell, Germany), pericyte (Cat No: C-28040, Promocell, Germany) and cardiomyocyte (Cat No: 05010,

STEMCELL, USA) differentiation media. The differentiation media were supplemented with 2% FBS and 1% Pen-Strep solutions and cells were maintained for 7 days. On day 4, autophagy was blocked/stimulated using 15 μ M HCQ and 50 μ M Met (Cat No: Osveh Pharmaceutical Inc., Iran) as previously described (Fig. 1A) [20].

2.6. Western blotting

Western blot analysis was done to evaluate and confirm the modulation of autophagy proteins in PC-, CM- and EC-like cells after the modulation of autophagy. On day 7, cells were collected and lysed in ice-cold cell lysis buffer solution (NaCl, NP-40, and Tris-HCl) enriched with cocktail enzyme inhibitors. Then, samples were sonicated at a resonance of 50 Hz for 2 minutes. The homogenates were centrifuged at 14,000 g for 20 minutes. By using the Picodrop spectrophotometer system (Model NO: PICOPET01; Serial NO: 000212/1), total protein content was determined in the supernatant. In this study, 100 μ g proteins from each sample were resolved by 12% SDS polyacrylamide gel electrophoresis and transferred to PVDF membrane. The membranes were incubated in antibody solution (LC3: Cat No: ab51520, Abcam; P62: Cat No: SC-10117; Santa Cruz Biotechnology, Inc.; Beclin-1: Cat No: SC-48341; Santa Cruz Biotechnology, Inc.; α -actinin-2: Cat No: SC-130928; Santa Cruz Biotechnology, Inc.; α -SMA: Cat No: SC-53015; Santa Cruz Biotechnology, Inc.; vWF: Cat No: SC-365712; Santa Cruz Biotechnology, Inc.; ERK 1/2: Cat No: SC-292838; Santa Cruz Biotechnology, Inc.; pERK 1/2: Cat No: SC-16981-R; Santa Cruz Biotechnology, Inc.) at 4 °C overnight. Then, the membranes were incubated with secondary HRP-conjugated anti-IgG antibody (Cat No: sc-2357; Santa Cruz Biotechnology, Inc.) for 1 hour at room temperature. The immunoreactive blots were detected using the ECL plus solution (BioRad). Immuno-reactive bands were analyzed with ImageJ software (ver.1.44p; NIH). GAPDH (Cat No: sc-32233; Santa Cruz Biotechnology, Inc.) was used as an internal control group. This experiment was performed in triplicate.

2.7. NO assay

The level of NO, either intracellular or released content, was measured in differentiating cells after autophagy stimulation or inhibition using the Griess method. In this method, NO is converted to nitrite and nitrite produces nitrous acid in an acidic state. In the next step, the addition of sulfanilamide to a solution containing nitrous acid forms a diazonium salt and in the presence of n-(1-naphthyl) ethylenediamine dihydrochloride ($C_{12}H_{16}Cl_2N_2$) generates an azo dye. Briefly, an initial number of 1×10^4 cells/well was seeded in each well of 96-well plates (SPL). 72 hours after the addition of autophagy blocker/stimulator under differentiation condition, 200 μ l supernatant of each sample was mixed with 20 μ l Griess A and maintained for 10 minutes followed by the addition of 20 μ l of Griess B solution. After 2 minutes, the optical density of each sample was read at 450 nm using a microplate reader (BioTek) and levels of NO calculated based on sodium nitrite standard curve. We also monitored the intracellular level of NO in addition to released content. Levels of NO were expressed as nM.

2.8. Measuring fatty acid composition by GC

The lipid profile was analyzed by the GC technique as previously described [21]. The cellular lipid was extracted by using the Bligh-Dyer method and further esterified with methanol during acetyl chloride catalysis [22]. Methyl esters were introduced to the analyzing machine in order to determine the fatty acid composition. The fatty acid methyl ester derivatives were separated on a Teknokroma TR CN100 column (60 × 0.25 mm) using a Buck Scientific gas chromatograph (Model 610; SRI Instruments, Torrance, USA). Tridecanoic acid (13:0) was exploited as the internal control. Peak retention times in each group were compared to the peak of standards.

2.9. Measuring endothelial RTKs and pro-inflammatory cytokines

To determine the levels of inflammatory cytokines and RTKs during CD146⁺ differentiation into different lineages, we measured the levels of IL-6 (Cat No: DY206; R&D) and TNF- α (Cat No: DY210; R&D) in the supernatants by using ELISA according to manufacturer's recommendation. The angiogenic status of cells was further assessed by monitoring RTKs protein levels such as VEGFR-1 (Cat No: ab32152; Abcam), VEGFR-2 (Cat No: ab39256; Abcam), Tie-1 (Cat No: ab27851; Abcam), Tie-2 (Cat No: ab24859; Abcam) and Ang-1 (Cat No: 130-06; Peprotech) by ELISA assay provided by our group [23]. The final absorbance was recorded at 450 nm using a microplate reader (BioTek; USA). The concentration of each factor either in autophagy stimulated/inhibited and groups is calculated based on comparison to corresponding standard curves.

2.10. Assessing paracrine potency of CD146⁺ cells under the modulation of autophagy

To this end, we monitored AChE touted as an exosome marker protein. In brief, supernatants were discarded after the completion of the experimental procedure and replaced by incubation with culture medium containing 1% exosome-free FBS (Invitrogen) for 48 hours. Thereafter, 20 μ l culture medium was mixed with 500 μ l buffer solution containing pyrophosphate (75 mM) and potassium hexacyanoferrate (2 mM) (Cat No: BXC0801; bioexfars) for 5 minutes at RT. Finally, 100 μ l s-butyrylthiocholine iodide was added to each sample and absorbance read at 405 nm during three different intervals. Finally, the choline esterase activity was calculated by the following formula; Activity (U/l) = Δ Abs/min \times 65800

2.11. RT-PCR assay

After 7-day incubation with differentiation media and autophagy modulation, the total RNAs were isolated from each sample. To this end, cells were trypsinized and were washed with PBS. Then, 1 ml Ambion TRIzol buffer (Cat No: 15596-026; Invitrogen; USA) was added to cell pellets and agitated rigidly to homogenize the samples. Next, 200 μ l chloroform (Merck; Darmstadt; Germany) was added and samples centrifuged at 4 °C at 12000 rpm for 20 minutes. Next, the equal volume of the upper phase containing RNA was mixed with isopropanol (Sigma-Aldrich) and incubated at 4 °C for 15 minutes. After centrifugation, the supernatant was discarded and the pellet was dissolved in 1 ml ethanol (75% v/v) solution. Finally, the total RNA was dissolved in 50 μ l DEPC treated water and samples' concentration

determined by a Nanodrop system (Thermo Scientific). To exclude a possible genomic DNA contamination, RNA solutions were incubated with the DNase1 kit (Cat No: en0521; Fermentaz). Before real-time PCR analysis, purified RNAs were reversely transcribed using a cDNA synthesis kit (Cat No: YT4500). The qRT-PCR reaction was performed by using 1 μ l cDNA, 5 μ l SYBR premix Ex Taq kit (Cat No: RR820L; TaKaRa), 0.4 μ l candidate gene primers and 3.2 μ l DEPC water. The qRT-PCR was performed by a Rotor-Gene Corbett System 6000. The raw data was analyzed by a convenient Pfaffl method with normalization to housekeeping gene β 2-microglobulin (β_2 M). The experiment was conducted in triplicate. The sequences of all primers for human VE-cadherin, cTnI, α -SMA, and TPBG were outlined in Table 1.

Table 1
The list of primers designed by Perl Primer software

Gene	Forward	Reverse	Tm (°C)
α -SMA	5'-GTCCACCGCAAATGCTTCTA-3'	5'-AAACACATAGGTAACGAGTCAG-3'	57
VE-cadherin	5'-ACCCAAGATGTGGCCTTTAG-3'	5'-GTGACAACAGCGAGGTGTAA-3'	60
Troponin I	5'-TTTGACCTTCGAGGCAAGTTT-3'	5'-CCCGGTTTTCTTCTCGGTG-3'	57
β 2M	5'-AGGCTATCCAGCGTACTCC-3'	5'-ATGTCGGATGGATGAAACCC-3'	58
CD63	5'-TCCTGAGTCAGACCATAATCC-3'	5'-GATGGCAAACGTGATCATAAG-3'	63
ALIX	5'-CTGGAAGGATGCTTTCGATAAAGG-3'	5'-AGGCTGCACAATTGAACAACAC-3'	63
Rab11	5'-CCTCAGCCTCTACGAAGCAAA-3'	5'-CCGGAAGTTGATCTCCTCCTG-3'	59
Rab27a	5'-AGAGGAGGAAGCCATAGCAC-3'	5'-CATGACCATTTGATCGCACCAC-3'	59
Rab27b	5'-GGAAGTGGCTGACAAATATGG-3'	5'-CAGTATCAGGGATTTGTGTCTT-3'	59

2.12. Statistical analysis

In this study, data are expressed as mean \pm SD. To find statistically significant differences between the groups, we performed a One-Way ANOVA test. $P < 0.05$ was considered statistically significant. Three sets of experiments were at least performed for different analyses unless mentioned.

3. Results

3.1. HCQ dose selection for the subsequent analyses

The optimum dosage of HCQ to inhibit autophagy was calculated based on the MTT assay. CD146⁺ cells were exposed to different doses of HCQ ranging from 2.5–20 µM for 3 days (Fig. 1B). According to our data, 3-day incubation of CD146⁺ cells with 2.5, 5 and 10 µM HCQ had no cytotoxic effect on cell survival rate. Data demonstrated that a slight increase in the cell survival rate from groups 2.5, 5 and 10 µM HCQ. The addition of 15 and 20 µM HCQ to the culture medium decreased cell viability to 98.3 and 82.7%, respectively, showing dose-dependent cytotoxicity of HCQ on the CD146⁺ cells (Fig. 1B). Consistent with the previous experiments, we selected 15 µM HCQ as the highest dose without toxic effect for other analyses [24].

3.2. HCQ treatment showed lysosomal accumulation inside the CD146⁺ cells

To further confirm the suppression of autophagy in CD146⁺ cells, the lysoTracker staining was done (Fig. 1C-E). According to results, the fluorescence intensity and the number of lysoTracker⁺ cells were increased in cells from 15 µM HCQ compared to the control non-treated cells ($p < 0.05$; Fig. 1C-E). We also found that the number of cells with accumulated lysosomes were increased in the 20 µM HCQ group compared to the control cells ($p < 0.05$; Fig. 1C-E). However, these effects were less compared to the 15 µM HCQ. We found a non-significant difference between groups 15 and 20 µM HCQ. These data showed that three-day incubation of CD146⁺ cells with HCQ at doses 15 and 20 µM HCQ could efficiently block autophagy efflux and accumulate lysosomes inside the CD146⁺ stem cells. According to data from MTT and IF assays, we selected 15 µM HCQ for subsequent analyses.

3.3. HCQ and Met changed protein levels of autophagy-related factors

Following the completion of the experimental protocol, we performed western blotting to measure protein levels of Beclin-1, P62 and LC3II/I ratio (Fig. 2A-B). According to our data, the treatment of CD146⁺ cells with the Met and endothelial differentiation medium significantly increased protein levels of P62 compared to the group treated with the HCQ group ($p < 0.05$). No statistically significant differences were found between the two groups for the Beclin-1 level and LC3II/I ratio ($p > 0.05$; Fig. 2A-B). The incubation of CD146⁺ cells with Met and cardiomyocyte differentiation medium increased Beclin-1 and LC3II/I ratio compared to the HCQ-treated cells ($p < 0.05$). However, the levels of P62 were decreased in Met-treated cells but did not reach statistically significant levels. We found a statistically non-significant difference in the protein levels of Beclin-1, P62 and LC3II/I ratio in CD146⁺ cells incubated with pericytes differentiation medium enriched with Met or HCQ (Fig. 2A-B). According to our data, one could hypothesize that the application of autophagy modulators (Met and HCQ) in CD146⁺ cells committed to different lineages changes the protein levels of autophagy-related proteins in a different manner, showing possibly different basal levels of autophagy function in different lineages.

3.3. NO production was increased after autophagy stimulation in differentiating cells

In order to monitor the level of NO production in differentiation cells subjected to autophagy modulation, we performed a Griess assay. Results indicated that intracellular NO content was diminished by autophagy suppression via 15 μ M HCQ compared to control-matched Met groups after incubation with cardiomyocyte, pericytes and endothelial cells differentiation medium ($p < 0.05$; Fig. 2C). The quantitative assessment of released NO in the supernatant medium showed that the levels of NO in the culture medium were more in groups PC and EC compared to the group CM (Fig. 2C). We also calculated the released/intracellular NO ratio, data showed that cells from EC had the potential to efficiently release NO to the supernatant exposed to 15 μ M HCQ compared to the Met-treated cells (Fig. 2C). These changes did not reach statistically significant in PC and CM groups. Overall, NO production was significantly hindered by autophagy inhibition while the stimulation of autophagy increases the NO production especially in CD146⁺ cells exposed to PC and EC differentiation media, showing NO production depends on the cell lineage.

3.4. HCQ and Met altered levels of differentiation-related proteins

We performed western blotting and real-time PCR analysis to assess the differentiation potential of CD146⁺ cells toward different lineages (Fig. 3A-B). Real-time PCR analysis showed that the treatment of CD146⁺ cells with autophagy modulators altered the expression of VE-cadherin, cTnI and α -SMA. According to our data, the incubation of CD146⁺ cells with Met significantly increased the expression of VE-cadherin, cTnI and α -SMA genes compared to the control and HCQ groups ($p < 0.05$; Fig. 3A). We found a significant inhibition of VE-cadherin in the group received HCQ compared to the control CD146⁺ cells ($p < 0.001$; Fig. 3A) while non-significant differences were found in the mRNA levels of both cTnI and α -SMA between the HCQ and control groups. These data demonstrated that the stimulation of autophagy signaling in CD146⁺ cells upon treatment with differentiation medium could increase differentiation potential toward multiple lineages. Western blotting showed that the modulation of CD146⁺ cells with autophagy modulators (either Met or HCQ) could promote lineage-specific protein synthesis compared to the control of CD146⁺ cells ($p < 0.05$; Fig. 3B). The protein analysis of VE-cadherin showed a significant increase in differentiating cells that committed endothelial lineage after exposure to the HCQ and Met. Of note, protein levels of α -SMA and vWF increased in CD146⁺ cells committed to pericyte and cardiomyocyte differentiation upon treatment with Met and HCQ. The levels of α -SMA and vWF reached significant levels in the differentiation medium enriched with Met and HCQ, respectively (Fig. 3B). Data revealed the significant phosphorylation of Erk1/2 in all cells exposed to differentiation media upon autophagy stimulation and inhibition ($p < 0.05$; Fig. 3B). Despite a slight increase in Erk1/2 phosphorylation of CD146⁺ cells exposed to pericyte lineage, these changes did not reach statistically significant differences.

3.5. Fatty acid profile was changed during the autophagy modulation in differentiating CD146⁺ cells

In the current experiment, we measured the level of PUFA (Linoleate 18:2 and Arachidonate 20:4), MUFA (Palmitoleate 16:1; Oleate 18:1) and SFA acids (Myristate 14:0, Pentadecanoic acid 15:0 and Palmitate 16:0 and Stearate 18:0) by GC analysis to monitor the ratio of unsaturated and saturated fatty acids in CD146⁺ cells exposed to autophagy stimulation and inhibition (Fig. 4). Data showed the increase of PUFA + MUFA: SFA ratio in CD146⁺ cells after the inhibition of autophagy by HCG. We found a 2.53-fold increase in the fatty acid ratio in the CM group exposed to 50 μ M Met compared to HCQ-treated CM during differentiation ($p < 0.05$; Fig. 4). Similar to the CM group, a 1.24-fold increase was found in the PUFA + MUFA/SFA ratio in PC after exposure to the Met in comparison with the HCQ. In contrast, we noted that the exposure of CD146⁺ cells to endothelial medium enriched with Met decreased this ratio (Fig. 4). Therefore, the application of autophagy modulators during differentiation of CD146⁺ cells toward different lineages such as EC, PC, and CM could alter the cellular fatty acid composition.

3.7. Autophagy modulation effect on RTKs levels and pro-inflammatory cytokines

Cell surface RTKs levels, VEGFR-1, VEGFR-2, Tie-1, Tie-2, and ligand Ang-1 were monitored by using ELISA. We found an increase in protein level for Tie-1, Tie-2, VEGFR-1 and VEGFR-2 under autophagy stimulation compared to the condition cells received HCQ (Fig. 5A). Despite slight changes, the protein levels of RTKs and Ang-1 did not reach statistically significant differences. In addition, it seems that autophagy modulation for 72 hours could not alter the potency of CD146⁺ cells to synthesize Ang-1 (Fig. 5A). To the assessment of the correlation between autophagy and the inflammatory process, we measured TNF- α and IL-6 (Fig. 5B). Data showed that autophagy induction by 50 μ M Met diminished either TNF- α or IL-6 levels in CD146⁺ cells incubated in EC and PC and CM differentiation media compared to the control-matched group exposed to the 15 μ M HCQ (Fig. 5B). According to data, we found that the CD146⁺ cells had a magnificent TNF- α and IL-6 synthesis capacity when committed to the endothelial lineage rather than pericyte and cardiomyocyte destination (Fig. 5B). Data showed that the promotion of autophagy by Met, although it did not, changes the RTKs and Ang-1 levels but could affect pro-inflammatory status via the reduction of TNF- α and IL-6 cytokines.

3.8. Autophagy modulation altered the exosome biogenesis

To further assess the modulation of autophagy on exosome biogenesis, AChE activity and the expression of genes including CD63, ALIX, Rab11, Rab27a, and Rab27b were measured. Data revealed the increase of exosome secretion to the supernatant in cells treated with HCQ compared to the Met groups (Fig. 6A). These data demonstrated that the treatment of CD146⁺ cells with autophagy blockers, 15 μ M HCQ, increases exosome abscission and activates paracrine activity. A similar pattern was found in the

expression of CD63, ALIX, Rab11, Rab27a, and Rab27b (Fig. 6B). In spite of induction in molecular pathways in exosomes biogenesis, localization and abscission of HCQ-treated cells, however, these changes did not reach statistically significant changes.

4. Discussion

The combinatorial cell therapy is touted as an intriguing approach to reach efficient results in terms of cardiac regeneration after myocardial infarction [25]. Therefore, the study of multiple differentiation capacity of distinct stem cells or progenitors could enable us in concomitant promotion of angiogenesis and cardiomyogenesis [26]. More than a decade, studies have suggested that different signaling pathways, such as autophagy, are involved to commence a novel cell-fate acquisition in different cell types [27]. Due to a lack of sufficient data, we reasoned that pharmacological modulation of autophagy (either stimulation or inhibition) in bone marrow-derived CD146⁺ cells would modulate the differentiation capacity and further change regenerative capacity. To this end, 72-hour incubation of CD146⁺ cells with 15 μ M HCQ revealed significant accumulation of intracellular vacuoles determined by LysoTracker staining, showing successful lysosomal dysfunction and autophagic inhibition [28]. In this study, we noted 72-hour incubation of differentiating CD146⁺ cells with 50 μ M Met induced protein synthesis of Beclin-1, and an increase in LC3-II/LC3-I ratio compared to the HCQ-treated groups. In contrast to CD146⁺ cells committed to endothelial lineage, a concurrent decrease in p62 in cells from PC and CM groups showed the completion of autophagic response after the exposure to the Met. While the current results showed contradictory P62 changes after autophagy modulation in progenitor cells oriented toward endothelial lineage. One reason for this discrepancy would be that the treatment of cells with lineage-specific factors could alter or blunt the normal function of the autophagic signaling pathway effector [29]. Therefore, one could hypothesize that the treatment of human bone marrow CD146⁺ cells could alter cellular levels of main autophagic regulators such as Beclin-1, P62 and LC3II/I ratio. Regarding the existence of diverse growth factors in differentiating media, it is logical to suppose that modulation of autophagy-related factors varies depending on the cell phenotype and activation of signaling pathways.

Interestingly, analysis of nitrosative stress showed significantly higher NO levels in groups treated with autophagy inhibitor HCQ compared to the Met-treated CD146⁺ cells. According to the results from the MTT test and NO analysis, it seems that 72-hour incubation of CD146⁺ cells with autophagy inhibitor committed to different lineages could reduce cell viability via the nitrosative stress [30]. Considering different levels of NO in EC, PC, and CM, it seems that progenitor cells respond differently to autophagy modulation upon differentiation to different lineages [31].

The differentiation capacity of CD146⁺ cells was also monitored after autophagy modulation. Real-time PCR analysis showed the potency of 50 μ M Met to up-regulate the mRNA expression of lineage-specific factors such as endothelial VE-cadherin, cardiac cTnI, and pericyte α -SMA compared to the control of CD146⁺ cells and HCQ-treated groups. Western blotting also exhibited an increase in protein levels of lineage-specific factors such as α -actinin, α -SMA, and vWF factor after modulation of autophagy

compared to the control group. These changes were in accordance with the phosphorylation of Erk1/2 in which groups received Met and HCQ showed a more Erk1/2 phosphorylation rate compared to the control cells [32]. According to the previous data, the modulation of autophagic response, either stimulation or inhibition, could induce the same enzymatic activity in different levels [32, 33]. The increase of cellular lineage-specific factors in HCQ-treated cells in comparison with control CD146⁺ cells could be related to the abolition of protein clearance after autophagy flux inhibition. However, more mechanistic investigations are needed to address the importance of autophagic status on the cellular distribution of specific factors.

We found that simultaneous autophagy modulation of human bone marrow CD146⁺ cells committed to PC, EC and CM lineages altered fatty acid profile in which an increased PUFA + MUFA/SFA ratio in Met-treated group was achieved compared to the HCQ counterpart. These data showed that the supplementation of differentiation culture medium with 50 µM Met shifted the differentiating CD146⁺ cells fatty acid profile from saturated to unsaturated status. Previous studies declared that the reduction of saturated fatty acids, notably palmitic acid, seems a strategic approach to increase autophagic flux [34]. This study showed the increase of MUFA and PUFA in differentiating CD146 cells after autophagic stimulation.

To find the possible cross-talk between the RTKs and autophagy status, we measured the levels of VEGFR-1, -2, Tie-1 and -2. Despite a slight increase in the level of VEGFR-1, -2, Tie-1 and -2 in cells exposed to the Met, these values did not reach statistically significant levels. Further analysis of CD146 cells after autophagy modulation showed a close interplay between autophagy and pro-inflammatory status [35]. We showed that the supplementation of differentiation media with 50 µM Met reduced inflammatory TNF-α and IL-6 production. Previous data confirmed that the promotion of autophagic response is a way to reduce pro-inflammatory status in the target cells [36]. The existence of the same pattern in the promotion of nitrosative status and inflammatory cytokine production could indirectly indicate that the inhibition of autophagy in progenitor cells could abort the survival rate after transplantation to the target sites [37].

We next went to define the interplay between the autophagy and paracrine activity in CD146 cells by monitoring the exosome secretion capacity. Our data showed the exosome secretion capacity indicated by supernatant AChE activity and stimulation of different genes involved in exosomes synthesis, transfer, and abscission in HCQ-treated cells. It seems that the inhibition of autophagy in differentiating cells promotes paracrine activity in vitro [38]. Commensurate with data from the current experiment and previous studies, it seems that the inhibition of autophagy and fatty acid change could alter the paracrine ability of progenitor and differentiating cells and increase of PUFA and MUFA is efficient in the secretion of exosomes [39].

Conclusion

In conclusion, it seems that the modulation of autophagy could alter the differentiation potential and exosome secretion of human CD146⁺ cells in vitro.

Abbreviations

3-(4, 5-dimethylthiazol-2-yl)-2,5-diphenyl tetrazolium bromide: MTT; 4', 6-Diamidino-2-Phenylindole: DAPI; Acetylcholine esterase: AChE; Alpha-smooth muscle actin: α -SMA; Angiopoietin-1 Ang-1; Cardiac troponin-I: cTnI; Cardiomyocytes: CMs; CD146: melanoma cell adhesion molecules; Chromatography: GC; Endothelial cells: ECs; Enzyme-linked immunosorbent assay: ELISA; Fetal bovine serum: FBS; Gas chromatography: GC; Hydroxychloroquine: HCQ; Interleukin 6: IL-6; Low-content glucose Dulbecco's Modified Eagle Medium: DMEM/LG; Magnetic Activated Cell Sorting: MACS; Metformin: Met; Mono Unsaturated Fatty Acid: MUFA; Mononuclear cells: MNCs; Pericytes: PCs; Phosphate-buffered saline solution: PBS; Poly Unsaturated Fatty Acid: PUFA; Reactive oxygen species: ROS; Real-time PCR: RT-PCR; Receptor Tyrosine Kinases: RTKs; Saturated Fatty Acid: SFA; Tumor necrosis factor alpha: TNF- α ; Tyrosine-protein kinase receptor-1: Tie-1; Tyrosine-protein kinase receptor-2: Tie-2; Vascular endothelial-cadherin: VE-cadherin; Vascular epithelial growth factor receptor-1: VEGFR-1; and Vascular epithelial growth factor receptor-2: VEGFR-2

Declarations

Availability of data and materials The datasets used and/or analyzed during the current study are available from the corresponding author on reasonable request.

Acknowledgements Authors thanks the stem cell Research Center personnel for guidance and help.

Funding This work was supported by grant (IR.TBZMED.REC.1397.636) from the Tabriz University of Medical Sciences.

Ethics declarations All procedures in this study were conducted in accordance with the European Medicines Agency's (EMA) pediatric committee (EudraCT number: 2011-004074-28) and conducted according to the 2000 revised principles of the Declaration of Helsinki (ClinicalTrials.gov identifier: NCT01765283). Written informed consent was obtained from the individuals.

Consent for publication None applicable

Competing interests Authors declare there is no conflict of interest

Author contribution M.H., J.R., and M.D., performed the experiments; A.H., collected the samples; R.R., M.N. supervised the study.

References

1. Mozaffarian D, Benjamin EJ, Go AS, Arnett DK, Blaha MJ, Cushman M et al. Heart disease and stroke statistics-2016 update a report from the American Heart Association. *Circulation*. 2016;133(4):e38-e48.
2. Gorjipour F, Hosseini-Gohari L, Alizadeh Ghavidel A, Hajimiresmaiel SJ, Naderi N, Darbandi Azar A et al. Mesenchymal stem cells from human amniotic membrane differentiate into cardiomyocytes and endothelial-like cells without improving cardiac function after surgical administration in rat model of chronic heart failure. *J Cardiovasc Thorac Res*. 2019;11(1):35-42. doi:10.15171/jcvtr.2019.06.
3. Katare R, Riu F, Mitchell K, Gubernator M, Campagnolo P, Cui Y et al. Transplantation of human pericyte progenitor cells improves the repair of infarcted heart through activation of an angiogenic program involving micro-RNA-132. *Circulation research*. 2011;109(8):894-906.
4. Avolio E, Meloni M, Spencer HL, Riu F, Katare R, Mangialardi G et al. Combined intramyocardial delivery of human pericytes and cardiac stem cells additively improves the healing of mouse infarcted hearts through stimulation of vascular and muscular repair. *Circulation research*. 2015;116(10):e81-e94.
5. Shaw I, Rider S, Mullins J, Hughes J, Péault B. Pericytes in the renal vasculature: roles in health and disease. *Nature Reviews Nephrology*. 2018;14(8):521.
6. Psaltis PJ, Simari RD. Vascular wall progenitor cells in health and disease. *Circulation research*. 2015;116(8):1392-412.
7. Avolio E, Madeddu P. Discovering cardiac pericyte biology: from physiopathological mechanisms to potential therapeutic applications in ischemic heart disease. *Vascular pharmacology*. 2016;86:53-63.
8. Cathery W, Faulkner A, Maselli D, Madeddu P. Concise review: the regenerative journey of Pericytes toward clinical translation. *Stem cells*. 2018;36(9):1295-310.
9. Herrmann M, Bara J, Sprecher C, Menzel U, Jalowiec J, Osinga R et al. Pericyte plasticity—comparative investigation of the angiogenic and multilineage potential of pericytes from different human tissues. *Eur Cell Mater*. 2016;31:236-49.
10. Frangogiannis NG. The Extracellular Matrix in Ischemic and Nonischemic Heart Failure. *Circulation research*. 2019;125(1):117-46.
11. Song S, Tan J, Miao Y, Li M, Zhang Q. Crosstalk of autophagy and apoptosis: Involvement of the dual role of autophagy under ER stress. *Journal of cellular physiology*. 2017;232(11):2977-84.
12. Miller BC, Zhao Z, Stephenson LM, Cadwell K, Pua HH, Lee HK et al. The autophagy gene ATG5 plays an essential role in B lymphocyte development. *Autophagy*. 2008;4(3):309-14.
13. Simon AK, Obba S, Zhang H, Riffelmacher T. *Autophagy in the Hematopoietic System*. American Society of Hematology Washington, DC; 2019.
14. Mizushima N, Levine B. Autophagy in mammalian development and differentiation. *Nature cell biology*. 2010;12(9):823-30.
15. Ke D, Ji L, Wang Y, Fu X, Chen J, Wang F et al. JNK1 regulates RANKL-induced osteoclastogenesis via activation of a novel Bcl-2-Beclin1-autophagy pathway. *The FASEB Journal*. 2019;33(10):11082-95.

16. Baerga R, Zhang Y, Chen P-H, Goldman S, Jin SV. Targeted deletion of autophagy-related 5 (atg5) impairs adipogenesis in a cellular model and in mice. *Autophagy*. 2009;5(8):1118-30.
17. Hou J, Han Z, Jing Y, Yang X, Zhang S, Sun K et al. Autophagy prevents irradiation injury and maintains stemness through decreasing ROS generation in mesenchymal stem cells. *Cell death & disease*. 2013;4(10):e844-e.
18. Zhang J, Liu J, Liu L, McKeehan WL, Wang F. The fibroblast growth factor signaling axis controls cardiac stem cell differentiation through regulating autophagy. *Autophagy*. 2012;8(4):690-1.
19. Ye H, Chen M, Cao F, Huang H, Zhan R, Zheng X. Chloroquine, an autophagy inhibitor, potentiates the radiosensitivity of glioma initiating cells by inhibiting autophagy and activating apoptosis. *BMC neurology*. 2016;16(1):178.
20. Zolali E, Rezaabakhsh A, Nabat E, Jaber H, Rahbarghazi R, Garjani A. Metformin Effect on Endocan Biogenesis in Human Endothelial Cells Under Diabetic Condition. *Archives of medical research*. 2019;50(5):304-14.
21. Mohammadzadeh F, Mosayebi G, Montazeri V, Darabi M, Fayezi S, Shaaker M et al. Fatty acid composition of tissue cultured breast carcinoma and the effect of stearoyl-CoA desaturase 1 inhibition. *Journal of breast cancer*. 2014;17(2):136-42.
22. Ulmer CZ, Jones CM, Yost RA, Garrett TJ, Bowden JA. Optimization of Folch, Bligh-Dyer, and Matyash sample-to-extraction solvent ratios for human plasma-based lipidomics studies. *Analytica chimica acta*. 2018;1037:351-7.
23. Hassanpour M, Rezaabakhsh A, Rahbarghazi R, Nourazarian A, Nouri M, Avci ÇB et al. Functional convergence of Akt protein with VEGFR-1 in human endothelial progenitor cells exposed to sera from patient with type 2 diabetes mellitus. *Microvascular research*. 2017;114:101-13.
24. Vijayaraghavan S, Karakas C, Doostan I, Chen X, Bui T, Yi M et al. CDK4/6 and autophagy inhibitors synergistically induce senescence in Rb positive cytoplasmic cyclin E negative cancers. *Nature communications*. 2017;8:15916.
25. Huang P, Wang L, Li Q, Xu J, Xu J, Xiong Y et al. Combinatorial treatment of acute myocardial infarction using stem cells and their derived exosomes resulted in improved heart performance. *Stem cell research & therapy*. 2019;10(1):1-12.
26. Reddy LVK, Sen D. Regulation of Cardiomyocyte Differentiation, Angiogenesis, and Inflammation by the Delta Opioid Signaling in Human Mesenchymal Stem Cells. *Regenerative Engineering and Translational Medicine*. 2019;5(3):252-62.
27. Hassanpour M, Rezaabakhsh A, Pezeshkian M, Rahbarghazi R, Nouri M. Distinct role of autophagy on angiogenesis: highlights on the effect of autophagy in endothelial lineage and progenitor cells. *Stem cell research & therapy*. 2018;9(1):305.
28. Amaravadi RK, Winkler J. Asymmetric bisaminoquinolines and bisaminoquinolines with varied linkers as autophagy inhibitors for cancer and other therapy. *Google Patents*; 2019.
29. Schaaf MBE, Houbaert D, Meçe O, To SK, Ganne M, Maes H et al. Lysosomal pathways and autophagy distinctively control endothelial cell behavior to affect tumor vasculature. *Frontiers in*

- oncology. 2019;9:171.
30. Rezaabakhsh A, Ahmadi M, Khaksar M, Montaseri A, Malekinejad H, Rahbarghazi R et al. Rapamycin inhibits oxidative/nitrosative stress and enhances angiogenesis in high glucose-treated human umbilical vein endothelial cells: role of autophagy. *Biomedicine & Pharmacotherapy*. 2017;93:885-94.
 31. Boya P, Codogno P, Rodriguez-Muela N. Autophagy in stem cells: repair, remodelling and metabolic reprogramming. *Development*. 2018;145(4):dev146506.
 32. Chen S-y, Chiu L-Y, Ma M-C, Wang J-S, Chien C-L, Lin W-W. zVAD-induced autophagic cell death requires c-Src-dependent ERK and JNK activation and reactive oxygen species generation. *Autophagy*. 2011;7(2):217-28.
 33. Mahli A, Saugspier M, Koch A, Sommer J, Dietrich P, Lee S et al. ERK activation and autophagy impairment are central mediators of irinotecan-induced steatohepatitis. *Gut*. 2018;67(4):746-56.
 34. Morselli E, Hernández-Cáceres MP, Toledo-Valenzuela L, Ávalos Y, Peña-Oyarzun D, Criollo A. Palmitic acid reduces the autophagic flux and insulin sensitivity through the activation of the free fatty acid receptor 1 (FFAR1) in the hypothalamic neuronal cell line N43/5. *Frontiers in Endocrinology*. 2019;10:176.
 35. Varga ZV, Giricz Z, Liaudet L, Haskó G, Ferdinandy P, Pacher P. Interplay of oxidative, nitrosative/nitrative stress, inflammation, cell death and autophagy in diabetic cardiomyopathy. *Biochimica et Biophysica Acta (BBA)-Molecular Basis of Disease*. 2015;1852(2):232-42.
 36. Ge Y, Huang M, Yao Y-m. Autophagy and proinflammatory cytokines: Interactions and clinical implications. *Cytokine & growth factor reviews*. 2018;43:38-46.
 37. Beljanski V, Grinnemo K-H, Österholm C. Pleiotropic roles of autophagy in stem cell-based therapies. *Cytotherapy*. 2019.
 38. Shrivastava S, Devhare P, Sujjantararat N, Steele R, Kwon Y-C, Ray R et al. Knockdown of autophagy inhibits infectious hepatitis C virus release by the exosomal pathway. *Journal of virology*. 2016;90(3):1387-96.
 39. Jackson CL. Membrane trafficking: a little flexibility helps vesicles get into shape. *Current Biology*. 2018;28(12):R706-R9.

Figures

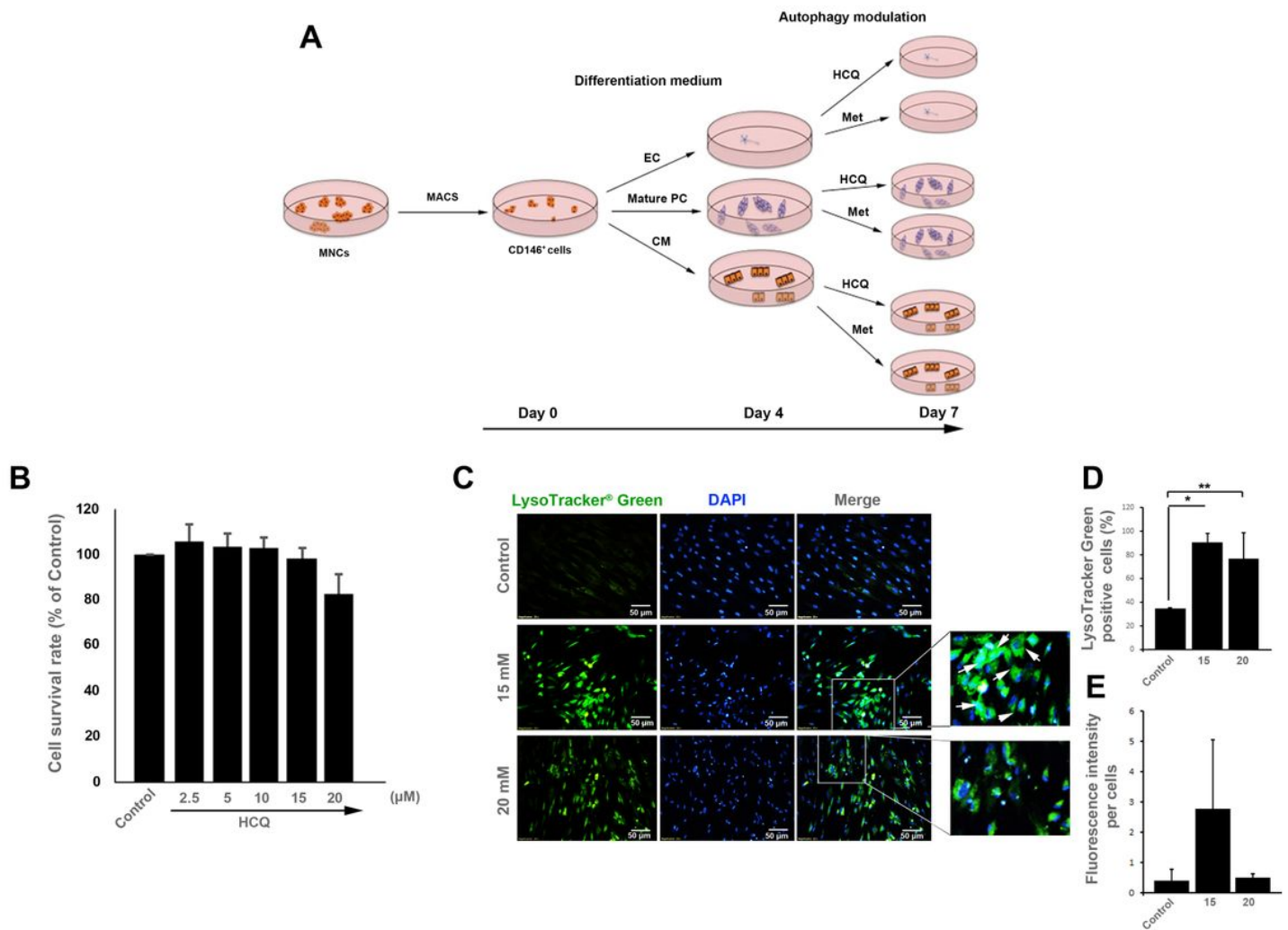


Figure 1

Schematic illustration of study design (A). Measuring CD146+ cell survival rate by MTT assay after exposure to different doses of HCQ (B; n=16). Our data illustrated that 15 μ M HCQ is the optimum dose for autophagy inhibition in CD146+ cells with a minimal toxic effect. Fluorescence microscopy imaging confirmed that 15 μ M HCQ inhibited autophagic flux (C; D (n= 100 cells); and E (n=100 cells)). Data are expressed as mean \pm SD. One-Way ANOVA and Tukey posthoc test. *p<0.05; **p<0.01

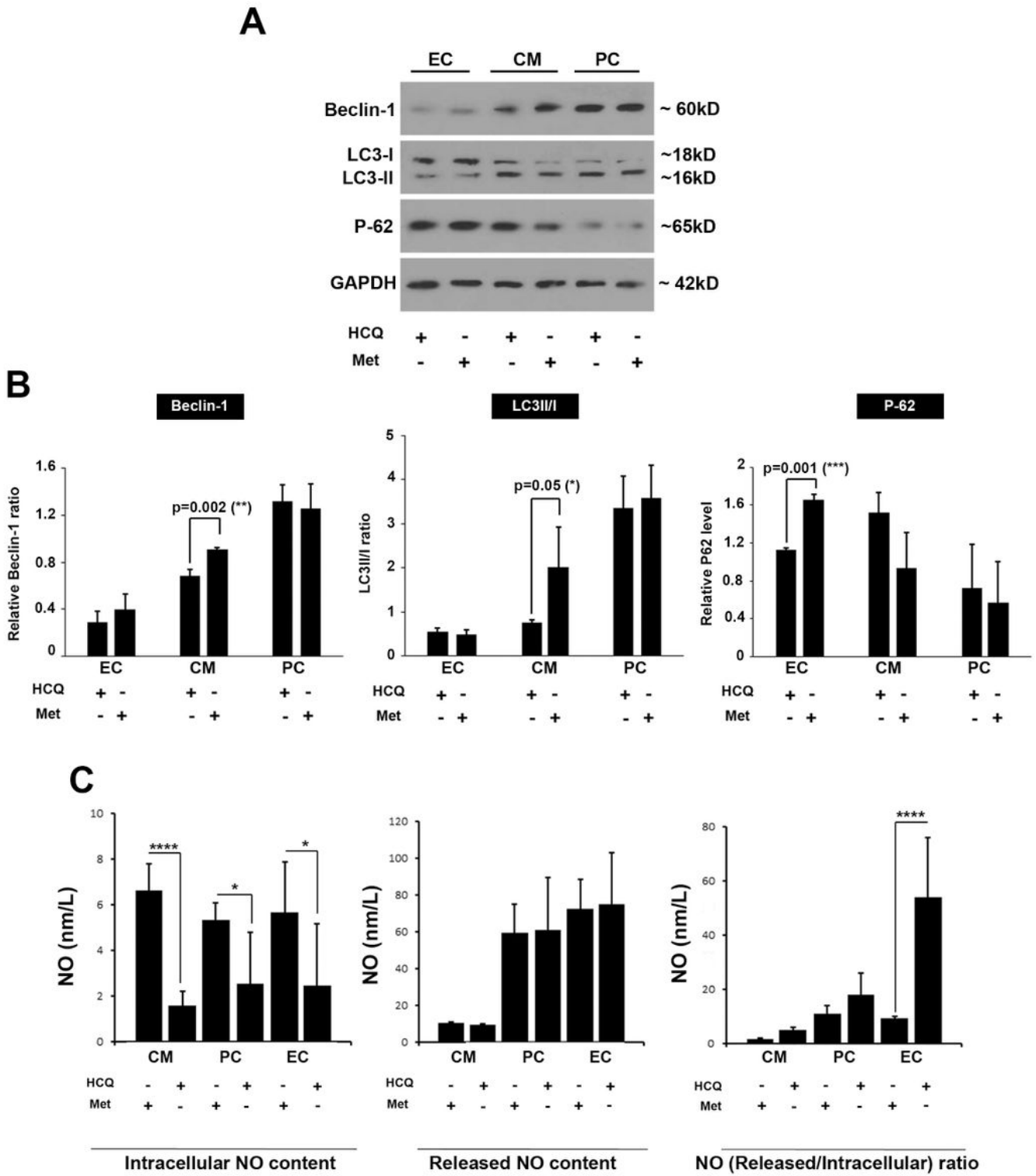
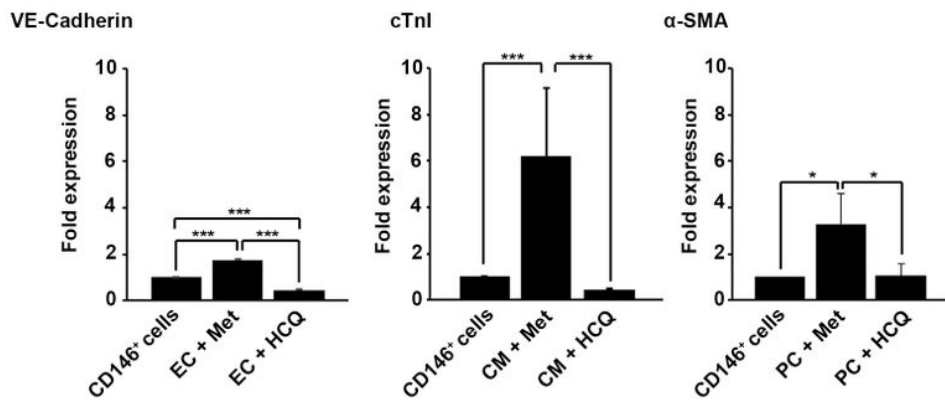


Figure 2

Measuring protein levels of autophagy-related factors by Western blotting (A and B; n=3). Detecting NO levels by Griess assay (C; n=16). Data are expressed as mean \pm SD. One-Way ANOVA and Tukey posthoc test. *p<0.05; ****p<0.0001

A



B

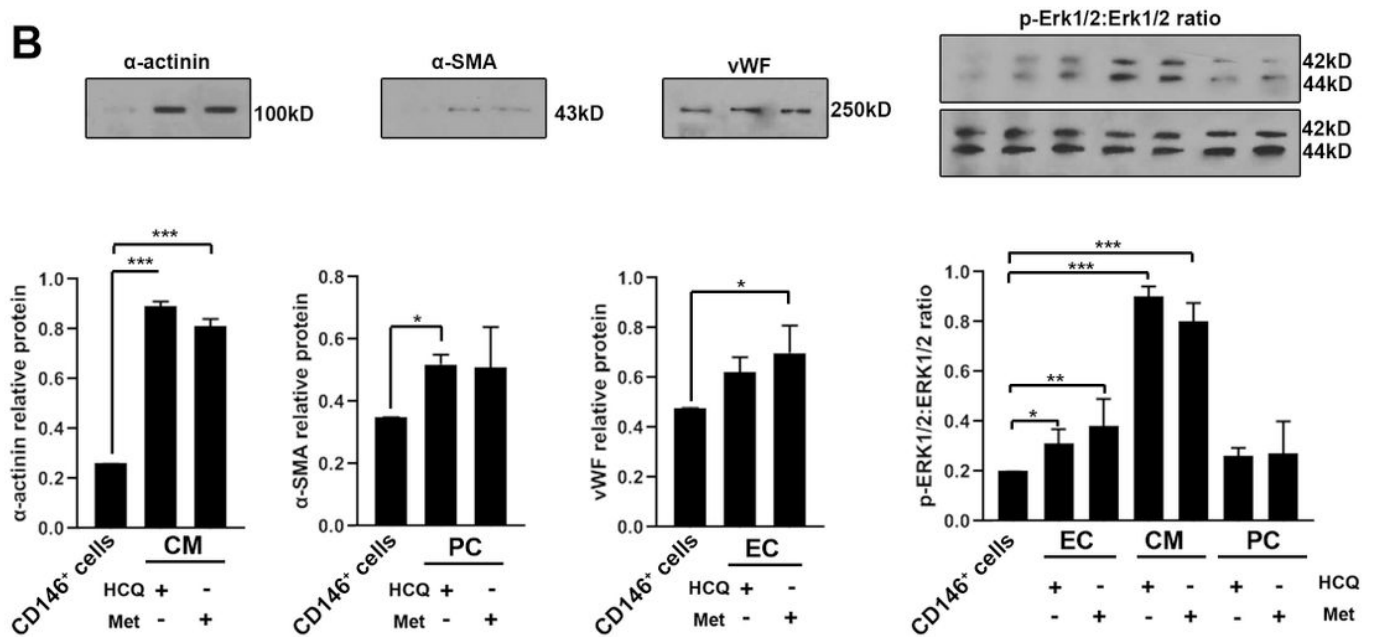


Figure 3

Measuring the effect of autophagy modulation on the differentiation capacity of human bone marrow CD146+ cells via real-time PCR assay (A; n=3). Data demonstrated that autophagy stimulation increased the mRNA level of endothelial VE-Cadherin, cardiac cTnI, and pericyte α-SMA after autophagy stimulation compared to non-treated CD146+ cells (A). Western blotting assays were used to monitor lineage protein levels after autophagy modulation (B; n=3). One-Way ANOVA and Tukey posthoc test. *p<0.05; **p<0.01; ***P<0.001; and ****p<0.0001

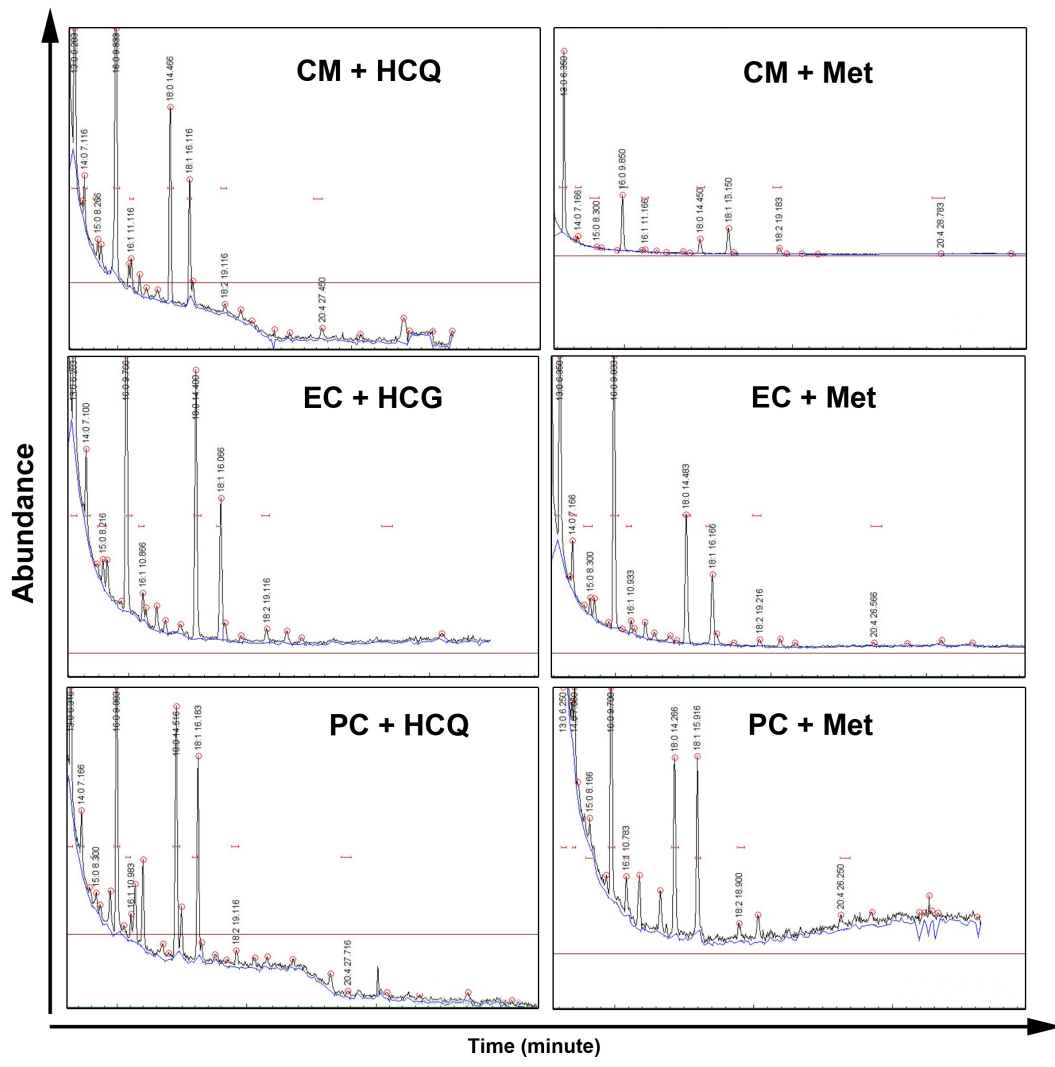
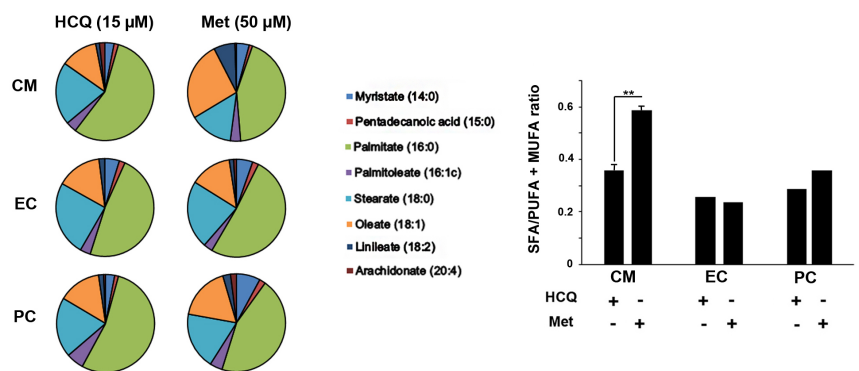
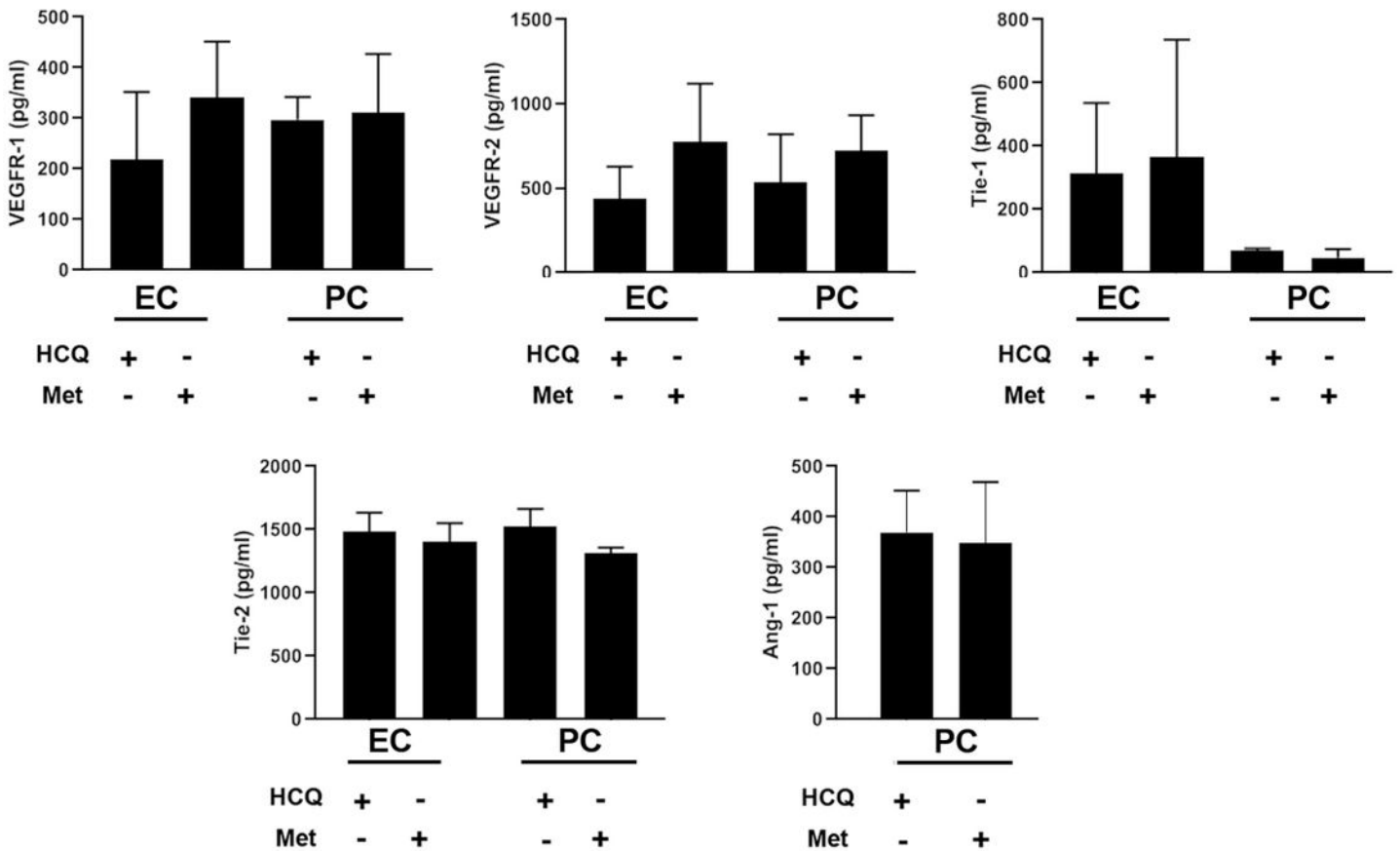


Figure 4

Gas chromatography fatty acids analysis indicated that the ratio of PUFA + MUFA/SFA was increased after autophagy stimulation in the CM group (n=3). Student t-test. **p<0.01.

A



B

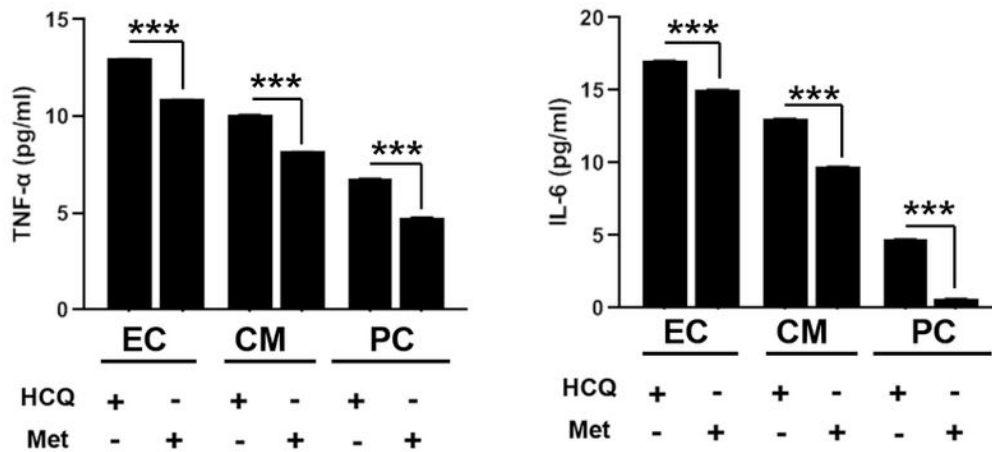


Figure 5

Measuring protein levels of VEGFR-1, VEGFR-2, and Tie-1, Tie-2 and Ang-1 after autophagy modulation (A; n=3). It seems that autophagy stimulation could increase differentiation potential but these changes did not reach statistically significant levels. The effect of autophagy stimulation/inhibition on the inflammatory status of differentiating CD146+ cells (B; n=3). It seems that autophagy stimulation could

decrease significantly the production of TNF- α and IL-6 after treatment with 50 μ M Met. Student t-test. ***P<0.001

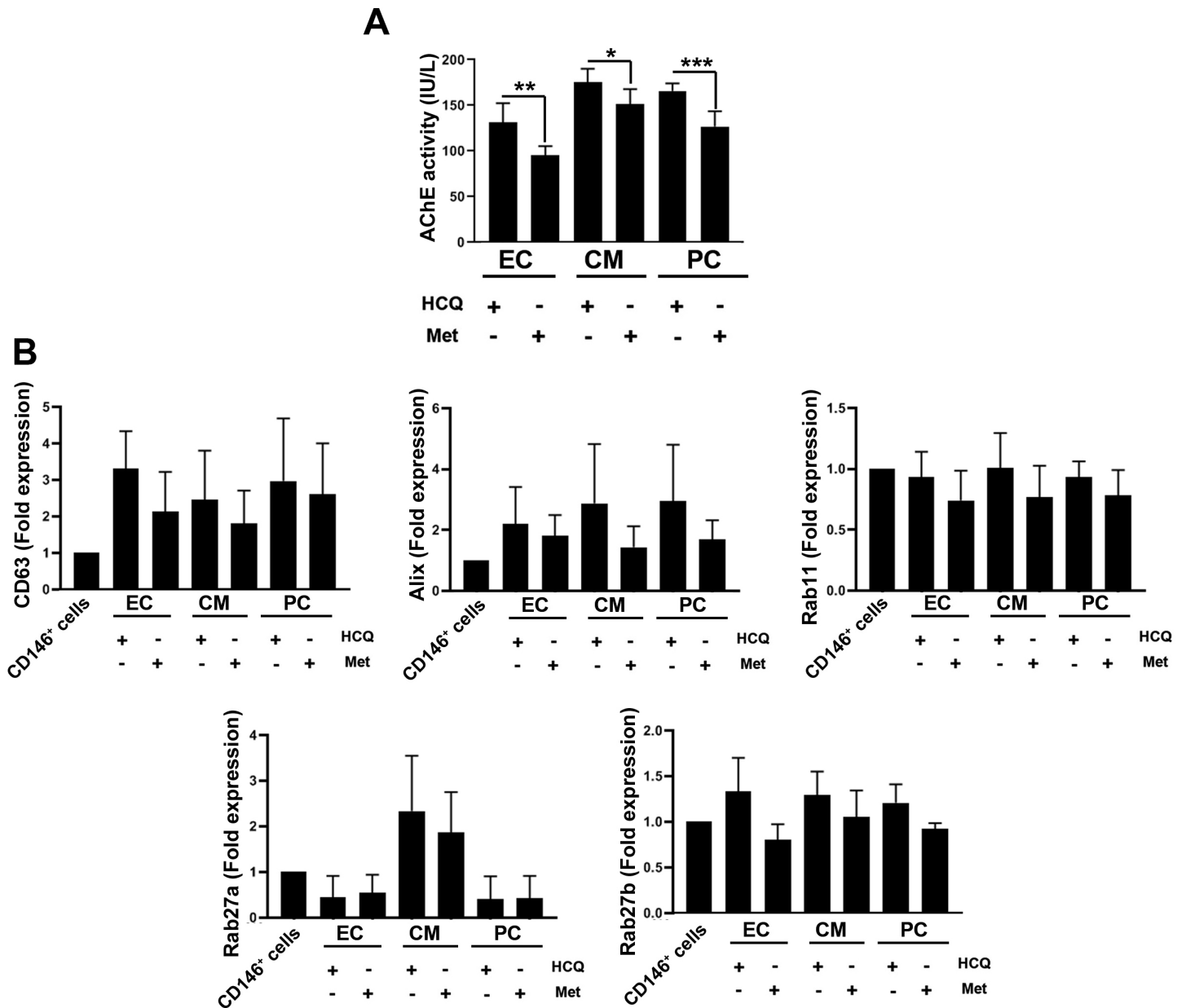


Figure 6

Evaluation of Interplay between autophagy and exosome biogenesis (A and B). Measuring AChE in supernatant cell culture (A). Data showed that autophagy stimulation by Met decreased AChE activity compared to the HCQ groups. Real-time PCR analysis revealed the expression of CD63, Alix, Rab11, Rab27a, and Rab27b in stimulated autophagy groups compared to HCQ-treated cells (B; n=3). These values did not reach significant levels. Student t-test. *p<0.05; **p<0.01; ***p<0.001